

## Simultaneously Enhancing Spectral Resolution and Sensitivity in Heteronuclear Correlation NMR Spectroscopy\*\*

Liladhar Paudel, Ralph W. Adams, Péter Király, Juan A. Aguilar, Mohammadali Foroozandeh, Matthew J. Cliff, Mathias Nilsson, Péter Sándor, Jonathan P. Waltho, and Gareth A. Morris\*

A method for acquiring pure shift heteronuclear single quantum correlation (HSQC) NMR spectra in real time is described. A windowed acquisition scheme consisting of trains of bilinear rotation decoupling (BIRD)<sup>[1,2]</sup> refocusing elements is used to acquire chunks of data with refocused  $J_{\text{HH}}$  modulation while suppressing  $J_{\text{XH}}$  with broadband heteronuclear decoupling. The resultant spectra show both enhanced resolution in  $F_2$  and enhanced signal-to-noise ratio.

Scalar spin–spin ( $J$ ) coupling provides valuable information for molecular structure elucidation, but the multiplet structure it causes is very expensive in terms of spectral resolution. In  $^1\text{H}$  NMR spectroscopy, multiplets are often many times the width of a single line. It is routine to suppress heteronuclear couplings ( $J_{\text{XH}}$ ) by broadband decoupling,<sup>[3–7]</sup> but only recently have experimental methods for homonuclear broadband decoupling become practical. These “pure shift” or “chemical-shift resolved” or “ $\delta$ -resolved” methods<sup>[8–19]</sup> can give resolution improvements approaching an order of magnitude, far in excess of any gains to be realistically expected from increases in the static magnetic field. However, all of these methods suffer to a greater or lesser extent from reduced sensitivity compared to conventional measurements. Here we describe an experimental method for obtaining pure shift heteronuclear single quantum correlation (HSQC) spectra, in which real-time homodecoupling using the BIRD pulse sequence element<sup>[1]</sup> leads to the first simultaneous resolution and signal enhancement in the directly detected ( $^1\text{H}$ ) dimension. (Homodecoupling has previously been described for the HSQC experiment, but only in the indirect ( $^{13}\text{C}$ ) dimension.<sup>[20]</sup>)

The HSQC experiment is the most widely used NMR method for correlating the chemical shifts of directly-bonded  $^{13}\text{C}$ – $^1\text{H}$  pairs. In its conventional<sup>[21]</sup> form, it shows proton multiplet structure in  $F_2$ , which limits resolution in the spectra of complex species. It has recently been shown<sup>[17,22,23]</sup> that it is possible to extend the pure shift methods currently used, which rely on stitching together separate measurements of short periods of decoupled signal, to real-time acquisition, in which homonuclear couplings are periodically refocused, by applying appropriate spin manipulations during the acquisition of a single free-induction decay. Such J-refocusing sequence elements are generally designed to be broadband, as distinct from classical selective<sup>[24,25]</sup> or band-selective<sup>[26]</sup> homodecoupling; in the case of HSQC, J-refocusing uses a BIRD pulse sequence element and a hard (nonselective)  $180^\circ$  pulse. The BIRD sequence element,<sup>[1]</sup> which, as its name suggests, was originally intended for broadband homonuclear decoupling, has, until recently,<sup>[12]</sup> been used almost exclusively for decoupling in the indirect dimension of heteronuclear 2D experiments.<sup>[27]</sup> Here, the combined effect of the BIRD sequence and the hard  $180^\circ$  pulse is to invert only those protons *not* directly coupled to  $^{13}\text{C}$ , thus refocusing the effects of couplings between the latter protons and protons that *are* directly coupled (bonded) to  $^{13}\text{C}$  and whose signals are recorded in HSQC. The great advantage of the BIRD method here is that, in contrast to Zangger–Sterk type methods,<sup>[8,9,22,23]</sup> it incurs no extra sensitivity penalty; indeed, the sensitivity is generally increased.

The BIRD sequence element has already been very effectively used to obtain pure shift  $^1\text{H}$ – $^{13}\text{C}$  HSQC spectra,<sup>[16]</sup> and pure shift 1D proton spectra of strongly coupled

[\*] Dr. L. Paudel, Dr. R. W. Adams, Dr. P. Király, Dr. J. A. Aguilar, Dr. M. Foroozandeh, Dr. M. Nilsson, Prof. G. A. Morris  
School of Chemistry, University of Manchester  
Oxford Road, Manchester, M13 9PL (UK)  
E-mail: g.a.morris@manchester.ac.uk  
Homepage: <http://nmr.chemistry.manchester.ac.uk>

Dr. P. Király  
Institute of Organic Chemistry, Hungarian Academy of Sciences  
Pusztaszeri út 59–67, 1025 Budapest (Hungary)

Dr. J. A. Aguilar  
Department of Chemistry, Durham University  
South Road, Durham, DH1 3LE (UK)

Dr. M. J. Cliff, Prof. J. P. Waltho  
Manchester Institute of Biotechnology  
131 Princess Street, Manchester, M1 7DN (UK)

Dr. M. Nilsson  
Department of Food Science, University of Copenhagen  
Rolighedsvej 30, 1958 Frederiksberg C (Denmark)

Dr. P. Sándor  
Agilent Technologies R & D a. Marketing GmbH & Co. KG  
Hewlett–Packard Strasse 8, 76337 Waldbronn (Germany)

[\*\*] This work was supported by the Engineering and Physical Sciences Research Council (EP/H024336/1, EP/I007989/1, and EP/E05899X/1), and by a UR Grant from the Agilent Technologies Foundation. P.K. thanks EMBO for a Short-Term Fellowship (ASTF 513-2012). Dr. A Hounslow kindly supplied assignments for the A $\beta$  peptide. Drs. P. Bowyer and W. Bermel provided useful comments regarding pulse sequence programming.

Supporting information for this article is available on the WWW under <http://dx.doi.org/10.1002/anie.201305709>.

© 2013 The Authors. Published by Wiley-VCH Verlag GmbH & Co. KGaA. This is an open access article under the terms of the Creative Commons Attribution License, which permits use, distribution and reproduction in any medium, provided the original work is properly cited.

species.<sup>[12]</sup> In both cases, the pure shift dimension was constructed from multiple separate acquisitions of short chunks of data, requiring ancillary software for the generation of decoupled spectra. Here we demonstrate how pure shift HSQC data with comparable resolution may be obtained much more quickly (to the point where a pure shift spectrum can require less time to acquire than a conventional spectrum) and without the need for any extra data processing. The one restriction is that the nucleus observed indirectly, generally <sup>13</sup>C, should not itself show homonuclear coupling; thus, for example, the proposed sequence is not suitable for fully <sup>13</sup>C-labeled compounds.

The pulse sequence used is shown in Figure 1. The initial part of the sequence is a conventional gHSQC,<sup>[21]</sup> with the

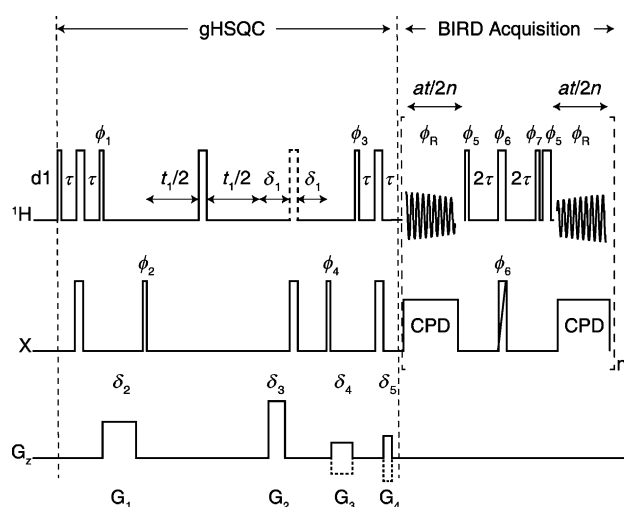


**Figure 1.** Pulse sequence for real-time pure shift gHSQC using BIRD. Narrow rectangles are 90° RF pulses, wide are 180° pulses, and wide with a diagonal line are either hard 180° pulses or composite 180° pulses. Gradient pulses G<sub>1</sub>–G<sub>4</sub> follow the normal pattern for gHSQC, and  $\tau = 1/(4^1 J_{XH})$ . The dotted proton RF pulse (0–2 times the duration of 90° pulse) centered between  $\delta_1$  delays is for multiplicity editing; for edited spectra this pulse is 180° and  $\delta_1 = 2\tau$ , which causes methylene protons to appear with opposite phase to methine and methyl; for unedited spectra this pulse is removed and  $\delta_1$  is set to  $\delta_2$  plus associated stabilization delay. The second  $\delta_1$  delay precedes a delay equivalent to a hard proton 180° pulse, which compensates for the evolution during the 180° pulse in middle of the  $t_1$  evolution. Each BIRD/180° J-refocusing block consists of a BIRD element, a hard 180° pulse, and a data acquisition window, with small delays (ca. 20  $\mu$ s) flanking the hard 180° proton pulse set to refocus the chemical shift. The first and last chunks are half in size ( $at/2n$ ) relative to the rest of the chunks ( $at/n$ ). Phase cycling:  $\phi_1 = [1\ 3]_4$ ,  $\phi_2 = [0\ 2]_2$ ,  $\phi_3 = [0\ 2]_8$ ,  $\phi_4 = [0\ 2]_{16}$ ,  $\phi_5 = [0\ 1]_2$ ,  $\phi_6 = [1\ 2]_2$ ,  $\phi_7 = [2\ 3]_2$ ,  $\phi_R = \{1\ 3\ 1\ 3\ (3\ 1\ 3\ 1)_2\ 1\ 3\ 1\ 3\ 1\ 3\ 1\ (1\ 3\ 1\ 3)_2\ 3\ 1\ 3\ 1\}$ , all other pulses are of phase 0 (for the explicit phase table, see Table S1).

double insensitive nuclei enhanced by polarization transfer (INEPT) followed by a windowed data acquisition, in which the effects of homonuclear coupling are periodically refocused. Applying  $n$  BIRD/180° J-refocusing elements during the acquisition time ( $at$ ) results in a free induction decay built up of an initial chunk of data of duration  $at/2n$ , ( $n-1$ ) chunks of duration  $at/n$ , and a final chunk of  $at/2n$ . Provided that  $n \gg (at \times J_{HH})$ , evolution under the homonuclear scalar coupling

can be neglected, although care is needed to ensure that chemical shift evolution is accurately refocused during the J-refocusing element. More frequent J-refocusing gives cleaner spectra, but at the expense of some extra line broadening owing to imperfect refocusing and T<sub>2</sub> relaxation. The BIRD real-time acquisition scheme differs slightly in timing from that previously proposed,<sup>[17]</sup> requiring fewer J-refocusing elements for a given spectral quality. Heteronuclear couplings are suppressed as usual by broadband irradiation (denoted CPD in Figure 1); the intermittent nature of the decoupling limits the types of modulation favored. Because BIRD selects protons directly bonded to <sup>13</sup>C, one class of coupling is not refocused, that between geminal protons. Spectra thus show singlet signals for all <sup>1</sup>H sites except for nonequivalent methylene protons, for which doublet signals are seen (full details of the sequence are given in the Supporting Information).

Figure 2 illustrates the application of the new real-time pure shift method to <sup>1</sup>H-<sup>13</sup>C correlated spectra. The conven-

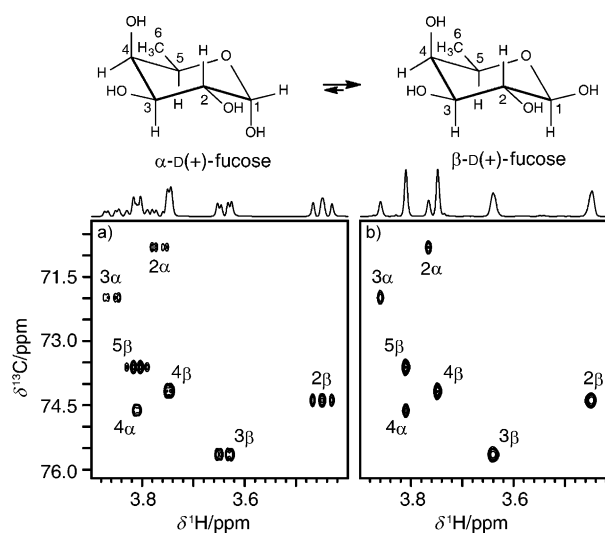


**Figure 2.** Selected regions (Indicated with dashed lines in the full spectra of Figure S1) of <sup>1</sup>H-<sup>13</sup>C HSQC spectra of D(+)-fucose in D<sub>2</sub>O with TSP as internal reference: a) conventional gHSQC; b) real-time pure shift gHSQC. 1D traces are integral projections onto the F<sub>2</sub> (<sup>1</sup>H) axis. Data were acquired, processed, and plotted with equivalent parameters, to allow quantitative comparison.

tional gHSQC spectrum (Figure 2a) of D(+)-fucose shows multiplet structure in the <sup>1</sup>H frequency (F<sub>2</sub>) dimension; the structure is collapsed to singlets in the pure shift spectrum (Figure 2b) obtained using the real-time pure shift gHSQC sequence of Figure 1. The 1D projections onto the <sup>1</sup>H (F<sub>2</sub>) axis show, as expected, that the singlets in the pure shift spectrum are more intense than the corresponding multiplets in the conventional HSQC. Peak heights increase by an average factor of 1.7 for doublets and 2.9 for multiplets. Linewidths in the pure shift spectrum are very similar to those in the conventional spectrum; although signal losses from imperfect pulses, mismatch between  $\tau$  and <sup>1</sup>J<sub>CH</sub>, and transverse relaxation should, in principle, lead to wider lines in the pure shift spectrum, for this example the degradation is negligible.

Similar results were obtained for quinine (Supporting Information, Figure S3); in this case the wider range of  $^{13}\text{C}$  chemical shifts means that some degradation in performance is seen at the edges of the spectrum. Any discontinuities in the decoupled signal, such as those caused by  $T_2$  relaxation during the BIRD sequence element, mismatch between the BIRD timing and  $^1J_{\text{CH}}$ , or a breakdown of the condition  $n \gg (at \times J_{\text{HH}})$ , will lead to small  $F_2$  sidebands at multiples of  $n/at$ . In the current work, the level of these sideband artifacts is typically around 1% (Figure S5).

The proposed method is also applicable to  $^1\text{H}$ - $^{15}\text{N}$  correlation, either at natural abundance or in labeled systems where the labels are too far apart for  $^{15}\text{N}$ - $^{15}\text{N}$  coupling to be significant (as is generally the case in peptides and proteins). Figure 3 compares conventional and real-time pure shift

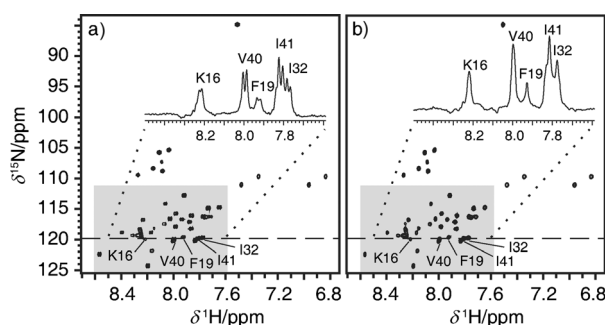


**Figure 3.**  $^1\text{H}$ - $^{15}\text{N}$  HSQC spectra of  $^{15}\text{N}$ -labeled A $\beta$  in  $[\text{D}_6]$ dimethylsulfoxide containing  $\text{H}_2\text{O}$  (5%): a) conventional gHSQC; b) real-time pure shift gHSQC. 1D spectra are corresponding  $^1\text{H}$  traces at  $\delta^{15}\text{N}$  of 119.7 ppm. All data were acquired, processed, and plotted with equivalent parameters, to allow quantitative comparison. Expansions from shaded regions are shown in Figure S6.

HSQC spectra for  $^{15}\text{N}$ -labeled beta-amyloid peptide 1-42 (A $\beta$ ). The shaded region in the conventional HSQC spectrum (Figure 3a) shows doublet resonances, which are collapsed to singlets in the pure shift HSQC spectrum (Figure 3b). As shown in the spectra, this collapsing of multiplets again improves both the resolution and sensitivity of the signals. Overcrowding in the shaded region is reduced; for example, with overlap between the signals of isoleucines 32 and 41 much reduced in the pure shift spectrum.

In conclusion, the pure shift gHSQC method described here leads to complete collapse of multiplet resonances into singlets (except for nonequivalent methylene signals, which collapse to doublets). This homonuclear decoupling produces signals with increased intensity and better resolution, lowering detection limits, speeding up experiments, and improving the ability to distinguish between signals in complex spectra. This method is potentially well-suited to automated spectral analysis, as a single signal is seen for each distinct chemical site or correlation.

### Experimental Section

All experimental data were obtained using a Varian VNMR5 500 MHz spectrometer equipped with a triple resonance ( $^1\text{H}/^{13}\text{C}/^{15}\text{N}$ ) triple axis gradient probe of maximum  $z$  gradient  $68.5 \text{ G cm}^{-1}$ ,

using GARP<sup>[5]</sup> heteronuclear decoupling ( $\gamma B_2/2\pi = 4.2 \text{ kHz}$  for  $^{13}\text{C}$ ,  $1.3 \text{ kHz}$  for  $^{15}\text{N}$ ) during data acquisition and BIP<sup>[28]</sup> composite pulses. The spectra in Figure 2 were acquired at  $20^\circ\text{C}$  using a  $100 \text{ mm}$  sample of D(+)-fucose in deuterium oxide, containing trimethylsilyl propionic acid (TSP) as internal reference. The unusually high concentration was used in order to confirm that clean results are obtainable, with artifact signals at around the 1% level. The following experimental and processing parameters were used: a hard  $90^\circ$   $^1\text{H}$  pulse of duration  $10.9 \mu\text{s}$ , a hard  $^{13}\text{C}$   $90^\circ$  pulse of duration  $15.2 \mu\text{s}$ , a BIP composite  $180^\circ$  pulse (for Figure 2b) of duration  $125 \mu\text{s}$  and bandwidth  $25 \text{ kHz}$ ; INEPT transfer delays  $\tau = 1.66 \text{ ms}$  and BIRD delays  $2\tau = 3.31 \text{ ms}$  (equivalent to  $^1J_{\text{CH}} = 151 \text{ Hz}$ ); homospoil gradient pulses of  $23.0 \text{ G cm}^{-1}$  ( $G_1$ ) and  $13.8 \text{ G cm}^{-1}$  ( $G_3$ ) of durations  $4.0 \text{ ms}$  ( $\delta_2$ ) and  $2.4 \text{ ms}$  ( $\delta_4$ ), respectively; and coherence selection (CTP) gradients of  $33.4 \text{ G cm}^{-1}$  ( $G_2$ ) and  $16.8 \text{ G cm}^{-1}$  ( $G_4$ ) of durations  $2.0 \text{ ms}$  ( $\delta_3$ ) and  $1.0 \text{ ms}$  ( $\delta_5$ ), respectively;  $^1\text{H}$  spectral width ( $sw$ ) was  $3592.0 \text{ Hz}$ ; 4 transients were averaged for each of  $2 \times 512$  free induction decays in which  $t_1$  was incremented to provide a  $^{13}\text{C}$  spectral width of  $11467.9 \text{ Hz}$  ( $swI$ ) in the  $F_1$  dimension; total number of points ( $np$ ) stored per FID was  $4104$ , and for Figure 2b  $n$  was  $27$ . Data were zero filled to  $16384 \times 8192$ , and Gaussian weighting was applied before double Fourier transformation. The total experiment times were  $4.2 \text{ h}$  for Figure 2a and  $4.4 \text{ h}$  for Figure 2b, the slightly greater duration for the latter arising from the  $27$  extra BIRD/ $180^\circ$  elements in each FID.

For Figure 3, data were acquired at  $25^\circ\text{C}$  using a solution of  $^{15}\text{N}$ -labeled A $\beta$  in  $[\text{D}_6]$ dimethylsulfoxide containing  $\text{H}_2\text{O}$  (5%). Experimental and processing parameters were: a hard  $90^\circ$   $^1\text{H}$  pulse of duration  $12.8 \mu\text{s}$ , a hard  $^{15}\text{N}$   $90^\circ$  pulse of duration  $44 \mu\text{s}$ , a BIP composite  $180^\circ$  pulse (for Figure 3b) of duration  $400 \mu\text{s}$  and bandwidth  $6.5 \text{ kHz}$ ; INEPT transfer delays  $\tau = 2.78 \text{ ms}$  and BIRD delays  $2\tau = 5.56 \text{ ms}$  (equivalent to  $^1J_{\text{NH}} = 90 \text{ Hz}$ ); homospoil gradient pulses of  $23.0 \text{ G cm}^{-1}$  ( $G_1$ ) and  $13.8 \text{ G cm}^{-1}$  ( $G_3$ ) of durations  $4.0 \text{ ms}$  ( $\delta_2$ ) and  $2.4 \text{ ms}$  ( $\delta_4$ ), respectively; and coherence selection (CTP) gradients of  $33.4 \text{ G cm}^{-1}$  ( $G_2$ ) and  $16.9 \text{ G cm}^{-1}$  ( $G_4$ ) of durations  $2.0 \text{ ms}$  ( $\delta_3$ ) and  $0.4 \text{ ms}$  ( $\delta_5$ ), respectively;  $^1\text{H}$  spectral width ( $sw$ ) was  $10.0 \text{ kHz}$ ; 32 transients were averaged for each of  $2 \times 64$  free induction decays in which  $t_1$  was incremented to provide a  $^{15}\text{N}$  spectral width of  $3.0 \text{ kHz}$  ( $swI$ ) in the  $F_1$  dimension; number of points ( $np$ ) sampled per FID was  $4096$ , and for Figure 3b  $n$  was  $8$ . Data were zero filled to  $16384 \times 512$  and then Fourier transformed without weighting. The total experiment time was approximately  $2.7 \text{ h}$  in each case.

Received: July 2, 2013

Published online: September 6, 2013

**Keywords:** bilinear rotation decoupling · gHSQC · homonuclear decoupling · NMR spectroscopy · structure elucidation

- [1] J. R. Garbow, D. P. Weitekamp, A. Pines, *Chem. Phys. Lett.* **1982**, *93*, 504–509.
- [2] D. Uhrin, T. Liptaj, K. E. Kövér, *J. Magn. Reson. Ser. A* **1993**, *101*, 41–46.
- [3] M. H. Levitt, R. Freeman, T. Frenkiel, *J. Magn. Reson.* **1982**, *47*, 328–330.
- [4] A. J. Shaka, J. Keeler, T. Frenkiel, R. Freeman, *J. Magn. Reson.* **1983**, *52*, 335–338.
- [5] A. J. Shaka, P. B. Barker, R. Freeman, *J. Magn. Reson.* **1985**, *64*, 547–552.
- [6] R. Fu, G. Bodenhausen, *Chem. Phys. Lett.* **1995**, *245*, 415–420.
- [7] E. Kupče, R. Freeman, *J. Magn. Reson. Ser. A* **1995**, *115*, 273–276.
- [8] K. Zangger, H. Sterk, *J. Magn. Reson.* **1997**, *124*, 486–489.

- [9] M. Nilsson, G. A. Morris, *Chem. Commun.* **2007**, 933–935.
- [10] G. A. Morris, J. A. Aguilar, R. Evans, S. Haiber, M. Nilsson, *J. Am. Chem. Soc.* **2010**, *132*, 12770–12772.
- [11] J. A. Aguilar, S. Faulkner, M. Nilsson, G. A. Morris, *Angew. Chem.* **2010**, *122*, 3993–3995; *Angew. Chem. Int. Ed.* **2010**, *49*, 3901–3903.
- [12] J. A. Aguilar, M. Nilsson, G. A. Morris, *Angew. Chem.* **2011**, *123*, 9890–9891; *Angew. Chem. Int. Ed.* **2011**, *50*, 9716–9717.
- [13] J. A. Aguilar, A. A. Colbourne, J. Cassani, M. Nilsson, G. A. Morris, *Angew. Chem.* **2012**, *124*, 6566–6569; *Angew. Chem. Int. Ed.* **2012**, *51*, 6460–6463.
- [14] A. J. Pell, R. A. E. Edden, J. Keeler, *Magn. Reson. Chem.* **2007**, *45*, 296–316.
- [15] A. J. Pell, J. Keeler, *J. Magn. Reson.* **2007**, *189*, 293–299.
- [16] P. Sakhaii, B. Haase, W. Bermel, *J. Magn. Reson.* **2009**, *199*, 192–198.
- [17] A. Lupulescu, G. L. Olsen, L. Frydman, *J. Magn. Reson.* **2012**, *218*, 141–146.
- [18] N. Giraud, M. Joos, J. Courtieu, D. Merlet, *Magn. Reson. Chem.* **2009**, *47*, 300–306.
- [19] M. Woodley, R. Freeman, *J. Magn. Reson. Ser. A* **1994**, *109*, 103–112.
- [20] M. Foroozandeh, P. Giraudeau, D. Jeannerat, *ChemPhysChem* **2011**, *12*, 2409–2411.
- [21] A. L. Davis, J. Keeler, E. D. Laue, D. M. Au, *J. Magn. Reson.* **1992**, *98*, 207–216.
- [22] R. W. Adams, J. A. Aguilar, G. A. Morris, M. Nilsson, L. Paudel, P. Sándor, 54<sup>th</sup> ENC Conference, Pacific Grove, CA, April 14–19, **2013**, Poster no. 360.
- [23] N. H. Meyer, K. Zangger, *Angew. Chem.* **2013**, *125*, 7283–7286; *Angew. Chem. Int. Ed.* **2013**, *52*, 7143–7146.
- [24] S. Alexander, *Rev. Sci. Instrum.* **1961**, *32*, 1066–1067.
- [25] A. G. Redfield, R. K. Gupta, *J. Chem. Phys.* **1971**, *54*, 1418–1419.
- [26] M. A. McCoy, L. Mueller, *J. Am. Chem. Soc.* **1992**, *114*, 2108–2112.
- [27] T. T. Nakashima, R. E. D. McClung in *Multidimensional NMR Methods for the Solution State* (Eds.: G. A. Morris, J. W. Emsley), Wiley, Chichester, **2010**, chap. 22, pp. 289–303.
- [28] M. A. Smith, H. Hu, A. J. Shaka, *J. Magn. Reson.* **2001**, *151*, 269–283.